J Mater Sci (2023) 58:4970–4986

Materials for life sciences

Can Synbone® cylinders and deer femurs reproduce ballistic fracture patterns observed in human long bones?

Nathalie Schwab[1,2], Xavier Jordana[1,3,4], Joan Soler[5], Xavier Garrido[5], Pedro Brillas[6], Andrés Savio[6,7], Santiago Lavín[8], Marisa Ortega-Sánchez[2,9], and Ignasi Galtés[1,2,3,10,*]

[1] *Unit of Biological Anthropology, Department of Animal Biology, Plant Biology and Ecology, Faculty of Biosciences, Universitat Autònoma de Barcelona, 08193 Bellaterra, Catalonia, Spain*

[2] *Forensic Pathology Service, Forensic Anthropology Unit, Catalonian Institute of Legal Medicine and Forensic Science (IMLCFC), Ciutat de la Justícia, Gran Via de les Corts Catalanes, 111 Edifci G, 08075 Barcelona, Spain*

[3] *Research Group of Biological Anthropology (GREAB), Biological Anthropology Unit, BABVE Department, Universitat Autònoma de Barcelona (UAB), Cerdanyola del Vallès, 08193 Bellaterra, Catalonia, Spain*

[4] *The Tissue Repair and Regeneration Laboratory (TR2Lab), University of Vic – Central University of Catalonia, Sagrada Família 7, 08500 Vic, Barcelona, Spain*

[5] *Mossos d'Esquadra, Unitat Central de Balística i Traces Instrumentals, Av. de la Pau, 12, 08206 Sabadell, Barcelona, Spain*

[6] *Donor Center Barcelona Tissue Bank (BTB), Hospital Clínic de Barcelona, C/Villarroel 170, Escala 12 Planta 4, 08036 Barcelona, Spain*

[7] *Banc de Sang i Teixits de Catalunya (BST), Pg. del Taulat, 116, 08005 Barcelona, Spain*

[8] *Servei d'Ecopatologia de Fauna Salvatge (SEFaS), Departament de Medicina i Cirurgia Animals, Facultat de Veterinària, Universitat Autònoma de Barcelona (UAB), Cerdanyola del Vallès, 08193 Bellaterra, Catalonia, Spain*

[9] *Anatomy and Embryology Unit, Morphological Sciences, Faculty of Medicine, Autonomous Universitat Autònoma de Barcelona (UAB), Cerdanyola del Vallès, 08193 Bellaterra, Catalonia, Spain*

[10] *Legal Medicine Unit, Department of Psychiatry and Legal Medicine, Universitat Autònoma de Barcelona (UAB), Cerdanyola del Vallès, 08193 Bellaterra, Catalonia, Spain*

Received: 29 November 2022
Accepted: 18 February 2023
Published online: 3 March 2023

ABSTRACT

Whereas gunshot injuries in human craniums have been well studied, reliable data on fracture patterns in ballistic long bone trauma remains scarce. Further information useful for forensic trauma interpretation and reconstruction may be retrieved from experimentally produced gunshot fractures. In order to avoid the use of human specimens for experimental research, it is of great interest to determine whether alternative models can reproduce the ballistic fracture patterns of human long bones. To address this question, we shot seven healthy adult human femurs and humeri each, ten samples each of two different polyurethane cylinders from Synbone® and four femurs from female red deer.

Handling Editor: Stephen Eichhorn.

Address correspondence to E-mail: ignasigaltes@gmail.com

https://doi.org/10.1007/s10853-023-08333-6

The specimens were embedded in ballistic gelatin and perpendicularly shot from a distance of 2 m, using a 9-mm full metal jacket projectile at an impact velocity of 360 m/s. The macroscopical appearance of the detailed fracture pattern considering entry, exit and general cortical traits as well as the bullet's energy lost upon impact were compared between the models. Despite some general similarities, neither of the two alternative models entirely reproduced the fracture patterns of human long bones. Comparing the two alternative models, the surrogate model revealed more significant differences to the human fracture than the animal model. This leads to the conclusion that the polyurethane material provides a different failure mechanism than real bone, underpinning the challenge in deploying an accurate analog.

Introduction

The analysis and reconstruction of gunshot wounds are frequent challenges in forensic medicine. Soft tissue injuries often show characteristic features, which allow conclusions about the applied mechanical force [1]. Examination of a well-preserved body differs widely from examination of corpses in poor condition such as those which are severely decomposed, burnt, scavenged, mummified or saponified [2]. Forensic evidence obtained from soft tissue in such conditions often remains inconclusive. The reconstruction of trauma and death may only be deduced from elements more resistant to destruction such as bone. Although signs of trauma almost always persist in bone, to date, reliable forensic conclusions have been very limited [3–5]. In particular, when fractured skeletal remains are shattered or incomplete, it can be challenging to clearly distinguish blunt force trauma from gunshot trauma [6, 7].

Forensic research on gunshot bone trauma has mainly focused on cranial injuries [8–10]. In contrast, only a few studies have dealt with gunshot trauma in long bones. In 1915, five types of ballistic fractures in human long bones have been described [11]. A bullet grazing a long bone may (1) produce a transverse fracture, (2) completely pierce the shaft, (3) become embedded in the bone, (4) strike the shaft and produce stellate or butterfly fractures and/or (5) break the bone into small fragments. Since then, most of the experimental studies with human bones focused on the fracture pathophysiology and risk prediction related to ballistic variables [12–16]. Apart from that research on ballistic trauma in human long bones mainly remained descriptive [17–21]. A recent review has summarized publications on ballistic fracture patterns observed in human long bones [22]. Therein, different types of fractures such as linear, oblique, comminuted and butterfly fractures are collated following direct gunshot trauma. However, detailed data on cortical fracture patterns of gunshot trauma in human long bones useful for forensic trauma interpretation and recreation are barely provided. To fill this gap of knowledge and incorporate confidence in gunshot trauma evaluation, experimental studies to reproduce ballistic fractures under controlled conditions are needed.

Since acquiring human material for experimental forensic research is not easy due to ethical barriers as well as complex tissue handling and preservation, there is growing interest in finding an alternative model for trauma experiments. A suitable analogue to replace human tissue for ballistic trauma recreations should feature a similar energy dispersion and fracture mode, despite the microstructural particularity of different materials.

In the past, both surrogate material and animal bones have been used for experimental ballistic research. Initially, polyurethane surrogates produced by Synbone® AG (Switzerland) were developed for surgical training. Due to the demand for an appropriate bone analogue for forensic testing and event recreation, the company has designed special models to react in the same way as bone during ballistic impact [23]. The surrogates are made from polyurethane and formed into different models to simulate gunshot trauma in various types of bone. Focusing on ballistic long bone trauma, few articles have been published using anatomical models or simplified cylinders from Synbone® [12, 24, 25]. According to Synbone® the latter were especially

designed for ballistic testing. In an experimental study from Henwood et al. [25], it was shown that the Synbone® cylinders behaved more like porcine bone than the anatomical Synbone® models. In contrast to the latter, the prior two presented comminuted fracture and a similar amount of the energy lost by the projectile upon impact. The authors claimed that the Synbone® cylinders may be used for ballistic impact tests to some extent, but drawing conclusions on fragment sizes or fracture propagation patterns were not recommended. However, these models were validated in comparison with porcine bone and not human bone.

Animal bones have played an important role in forensic experimental research too [24, 26–29]. However, there are morphological and biomechanical differences and no animal long bone consistently resembles the human. In terms of morphology and biomechanical properties, Kieser et al. [30] found deer femurs were the least dissimilar from human femurs compared to pig and sheep bones. In experimental studies, the same authors have used female deer femurs to produce remote and indirect ballistic fractures, whereby in both cases wedge-shaped fractures were reported [26, 27].

Nevertheless, in summary, detailed ballistic fracture patterns in different models have not been clearly defined yet. Thus, the query as to whether alternative surrogate and animal models are suitable to reproduce the fracture patterns of human long bones remains to be answered. To address this question, we experimentally inflicted gunshot trauma to human femurs and humeri, Synbone® surrogates and deer femurs. Qualitative and quantitative evaluation was made on all samples to compare the macroscopic fracture patterns.

Materials and methods

Samples and sample preparation

Human bones

The Donor Center-Barcelona Tissue Bank, department of Banc de Sang i Teixits de Catalunya provided 14 healthy, entire, unfractured, fresh human bones from cadavers with informed consent from their relatives. Seven femurs and humeri each were collected from a total of six male aged between 55 and 71 years.

With a postmortem time interval of up to 24 h the bones were dissected from the limbs, defleshed and stored in the freezer until further use. The human femurs had an average length of 46.1 cm (43–52 cm), an average mid-diaphyseal width of 2.9 cm (2.5–3.3 cm) and an average cortical thickness of 5.8 mm (5–6.5 mm). The human humeri had an average length of 32.6 cm (30.8–36.6 cm), an average mid-diaphyseal width of 2.1 cm (1.9–2.3 cm) and an average cortical thickness of 3.1 mm (3–4 mm).

Synbone® surrogates

Two different types of polyurethane cylinders from Synbone®, each ten, were selected. Both types have a length of 27 cm, an outer diameter of 3 cm, a hollow interior and are covered with a rubber skin simulating periosteum. Model PR0109.G is hereafter referred to as humerus cylinder and has a wall thickness of 3 mm, which is similar to the human humerus. Model PR0108.G is hereafter referred to as femur cylinder and has a wall thickness of 5 mm, which is similar to the human femur.

Animal bones

The Faculty of Veterinary of the Universitat Autònoma de Barcelona (UAB) provided four healthy, entire, undamaged, fresh femurs from wild-shot, young adult, female red deer (*Cervus elaphus*). The animals were shot for hunting reasons. The femurs were dissected with very little soft tissue attached, leaving the periosteum intact. They had an average length of 22.4 cm (21.6–23.3 cm), an average mid-diaphyseal width of 1.9 cm (1.8–2 cm) and an average cortical thickness of 3.8 mm (3.5–4 mm). They were stored in the freezer until further use.

Preparation of the ballistic gelatin blocks

All specimens were embedded in ballistic gelatin to simulate transparent soft tissue. We used gelatin from Clear Ballistics (Canada), which is supplied as a ready mixed, solid block that needs to be melted at 100 °C for 4–5 h before it can be individually applied. The liquid gelatin was poured into molds with the samples and left to solidify at air temperature overnight. The thickness of the gelatin on the target side

was 2 cm for each specimen. In case of the Synbone® cylinders, also the hollow interior was filled with gelatin to simulate bone marrow and its exploding reaction to gunshot [31, 32].

Shooting procedure

The 9 mm Luger test barrel (Drello Bal 1025 FU-R) was used to fire a 9 mm Luger full metal jacket projectile to each specimen. The impact velocity of the projectile was 360 m/s, simulating a shot from a handgun. The specimen blocks were placed 2 m before the muzzle. In order to ensure a perpendicular impact, we constructed a device that held the specimens at the ends to stabilize them upright. An optical laser was used to define the impact point in the middle of the shaft. For velocity measurement of the projectile upon impact, a light barrier (Drello LS 11-03) with a computerized system (Drello VC 4043-09) was used.

Sample assessment

After the shooting, the fractured samples were removed from the gelatin blocks. The synthetic periosteum of the Synbone® surrogates could be smoothly peeled off. In order to clean the human and animal bones, they were cooked at 100 °C in a water detergent solution (one cup of commercial degreasing detergent in 5 L of plain water) [33]. After 2–5 h of cooking, the bones were cleaned and left to dry. After the cleaning process, the fragments of each specimen were reassembled with a superglue to better visualize the fracture patterns.

All samples were macroscopically examined to define the fracture type and cortical fracture patterns. The latter was subdivided in entrance, exit and general cortical traits. We determined the fracture type by the appearance of the impact side. Furthermore, we counted the different forms of radiating fracture lines around the bullet entry: longitudinal (lines running along the longitudinal axis toward the epiphysis/cylinder ends), oblique (lines running at an angle to the longitudinal axis of the samples) and transverse (lines running horizontally from the entry point to the posterior aspect of the samples). Any fracture line longer than 5 mm was counted. For further quantitative analysis, the cortical thickness at the level of the impact, the maximal longitudinal fracture extent and the horizontal and vertical diameter of the bullets' entrance and exit hole were measured with a calliper. The measurement of the post-impact velocity of the projectiles allowed the calculation of the kinetic energy lost in each sample ($Ke = 0.5\ mv^2$). The mass (m) of the projectile was 7.98 g. After collection of all data, they were compared within the sample categories.

Statistics

Pearson's Chi-squared test was carried out to determine significant differences in the frequencies of the entry, exit and general cortical traits between the sample groups. Contingency coefficients were calculated to correlate the traits with the sample groups. The multivariate correspondence analysis was used to examine correlations and clusters between the fracture traits in the sample groups.

The quantitative variables such as entry and exit hole size, fracture extent, percentage of transverse fracture lines and energy loss values were tested for normality and equal variance using Shapiro Wilk and Levene's test. An analysis of variance using One-Way ANOVA was performed. Games-Howell post hoc test was applied to compare the quantitative variables between the sample groups. Significance level was set at 0.05.

Ethics

This study followed the ethical precepts of the Declaration of Helsinki (Fortaleza, Brazil, Oct 2013) and was approved by the local ethics committee (Bellvitge University Hospital, L'Hospitalet de Llobregat, Barcelona; Ref. PR416/20). Human samples were processed according to guidance for clinical use (EEC regulations 2004/23/CE and 2006/17/CE) and to the legal requirements of Spain (Law 14/2007, RD 1716/2011 and RD 9/2014). All human bone samples were donated anonymously and obtained under informed consent. The respective samples are stored in the private collection at the Catalonian Institute of Legal Medicine and Forensic Science (IMLCFC) in Barcelona, Spain (Registro Nacional de Biobancos. Ref. C.0004241).

Results

Qualitative fracture characteristics

All samples were completely perforated by the bullet and presented comminuted fractures. In the human bones and Synbone® cylinders the complete specimen length, the entrance and exit holes could be reconstructed. In contrast, the animal bones exhibited a massive fragmentation, particularly on the lateral aspects of the bullet perforation. This hampered the shaft assembling, allowing only a partial reconstruction of the entry and exit hole. All samples presented a various number of radiating fractures lines creating a stellate pattern at the impact side. Explanations of the assessed cortical traits are given below. We divided them into entrance, exit and general traits as shown in Table 1 (the wall of the surrogates will still be referred to as cortical for the sake of simplified readability). To the best of our knowledge, some of these traits have not yet been reported in the literature. In all sample groups we found the impact side provided more cortical characteristics to identify gunshot trauma than the exit.

Entrance traits (Figs. 1, 3)

A *round entry hole* is the bullets initial entry defect that visually appears round.

A *V-shape* of the bone is present proximal and/or distal of the entry hole. The tip of the V points toward the impact and the margins are defined by oblique fracture lines.

Y-branching is present proximal and/or distal of the entry hole. It is a bifurcation of the longitudinal fracture line into two oblique lines that run toward both lateral aspects.

Tip fragmentation is a superficial, external loss of cortical fragment(s) at the tip of the bone around the bullet entry. The transition to the intact cortical bone is sharply defined by quite chiseled edges. Tip fragmentation on bone pieces next to each other appears as a stepped circular margin around the entry.

Table 1 Cortical traits analyzed in all sample groups subdivided in entrance traits, exit traits, and general traits, with the respective x^2 test's *p*-value and contingency coefficient (CC)

	Human femur		Human humerus		Synbone® femur cylinder		Synbone® humerus cylinder		Deer femur		*p* value	CC
N	7		7		10		10		4			
Entrance traits												
Round hole	7	100%	7	100%	10	100%	10	100%	0	0%	< 0.001	0.707
V-shape	7	100%	7	100%	4	40%	7	70%	4	100%	0.011	0.506
Y-branching	0	0%	1	14%	7	70%	6	60%	0	0%	0.005	0.532
Tip fragmentation	6	86%	6	86%	6	60%	3	30%	4	100%	0.034	0.463
Wing flake	4	57%	2	29%	0	0%	0	0%	0	0%	0.006	0.524
Wing flake defect	6	86%	2	29%	0	0%	0	0%	0	0%	< 0.001	0.624
Ring defect	7	100%	7	100%	0	0%	1	10%	0	0%	< 0.001	0.688
Depressed ring	0	0%	0	0%	10	100%	10	100%	0	0%	< 0.001	0.707
Bullet wipe	0	0%	0	0%	10	100%	10	100%	0	0%	< 0.001	0.707
Internal beveling	7	100%	7	100%	10	100%	10	100%	4	100%		
Radiating Fx lines	7	100%	7	100%	10	100%	10	100%	4	100%		
Exit traits												
Round hole	1	14%	0	0%	2	20%	8	80%	0	0%	0.001	0.570
Square hole	6	86%	7	100%	8	80%	2	20%	0	0%	< 0.001	0.597
Layered breakage	7	100%	6	86%	0	0%	0	0%	0	0%	< 0.001	0.707
External beveling	7	100%	7	100%	9	90%	10	100%	4	100%	0.579	0.265
Radiating Fx lines	7	100%	7	100%	10	100%	10	100%	4	100%		
General traits												
Plastic deformation	7	100%	7	100%	0	0%	0	0%	4	100%	< 0.001	0.707
Wall splitting	2	29%	0	0%	9	90%	6	60%	0	0%	< 0.001	0.576

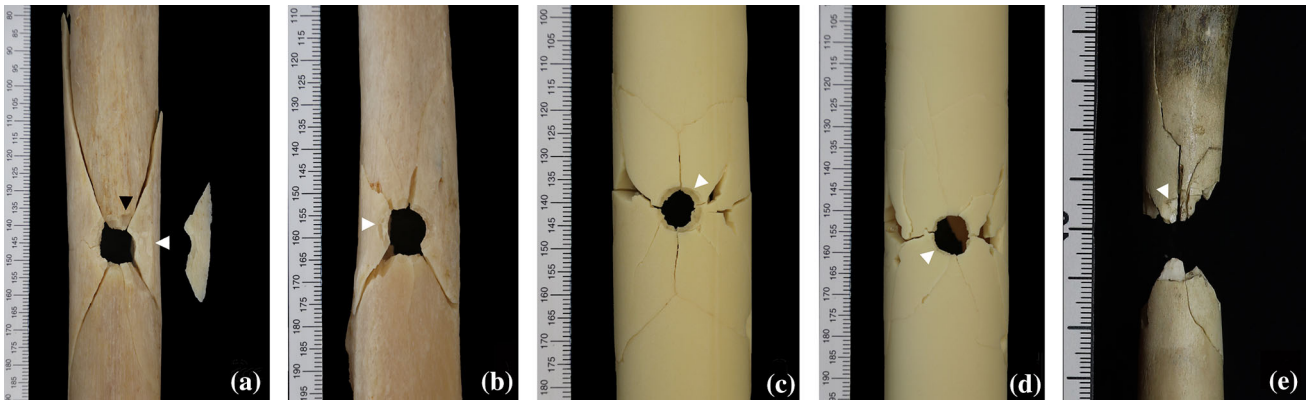

Figure 1 Stellate fracture at the impact side of a **a** human femur with a round entry hole surrounded by a partial ring defect, tip fragmentation (black arrow head), wing flake defect (white arrow head), wing flake and V-shape, **b** human humerus with a round entry hole surrounded by a partial ring defect (white arrow head) and V-shape, **c** Synbone® femur cylinder with a round entry hole surrounded by a depressed ring and bullet wipe (white arrow head) and Y-branching, **d** Synbone® humerus cylinder with a round entry hole surrounded by a depressed ring and bullet wipe (white arrow head) and V-shape, **e** deer femur with tip fragmentation (white arrow head) an V-shape.

A *wing flake* is a loose trapezoidal chip of cortical bone that resembles spread wings. It originates from the lateral aspect(s) of the entry hole.

A *wing flake defect* is the imprint of a wing flake that is left on the lateral aspect(s) of the entry hole.

A *ring defect* is a circular or partial circular loss of superficial cortical bone on the margin of the entry hole. Its appearance reminds of an abrasion ring. It may be interrupted by other entrance patterns such as tip fragmentation.

A *depressed ring* is a circular or partial circular depression of the entry hole margin.

A *bullet wipe* appears as a gray ring around the entry hole.

Internal beveling is a funnel shape in the cortical wall with the larger part on the internal aspect.

Radiating fracture lines run from the entry hole toward the epiphyses and the posterior aspect of the sample.

A significant difference was found for round entrance hole that was produced in all human bones and Synbone® surrogates, while in the deer femurs it could not be reconstructed. V-shape was featured by all human and animal bones and thus significantly more frequent than in Synbone® surrogates. Y-branching was significantly more often present in Synbone® surrogates than in human humeri, while in human and deer femurs it was never observed. Tip fragmentation was featured by all deer femurs and the majority of human bones and thus significantly more frequent than in the Synbone® surrogates. Also statistically significant were the findings wing flake and wing flake defect that exclusively occurred in human bones. Ring defect was statistically significant present in all human bones and in only one humerus cylinder from Synbone®, while in femur cylinders and deer femurs it was never observed. Finally, all Synbone® surrogates significatively featured depressed ring and bullet wipe, while in human and animal bones both traits were absent. No statistical significances were found for internal beveling and radiating fracture lines that both occurred in every specimen.

Exit traits (Figs. 2, 3)

Round exit hole is the bullets exit defect that visually appears round.

Square exit hole is the bullets exit defect that visually appears edgy or square.

Layered breakage is a layered pattern on the fracture surface of the cortical bone.

External beveling is a funnel shape in the cortical wall with the larger part on the external aspect.

Radiating fracture lines run from the exit defect toward the epiphyses and the anterior aspect of the sample.

Concerning the exit traits, all human humeri and the majority of the human femurs and femur cylinders showed a square exit hole. This is statistically significant compared to the humerus cylinders that mostly featured a round exit hole. As noted, the exit hole in deer bones could not entirely be

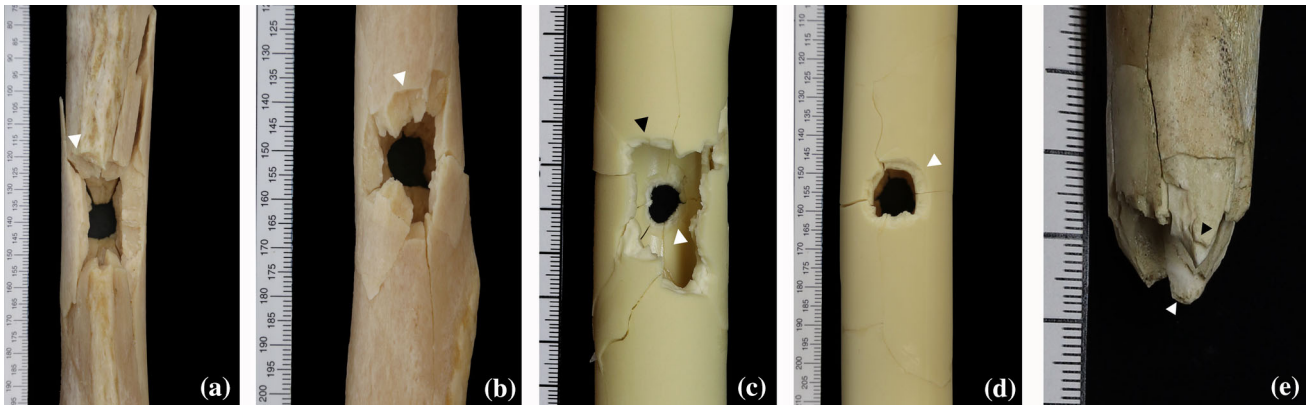

Figure 2 The exit side of a **a** human femur with a square exit hole and external beveling (white arrow head), **b** human humerus with a square exit hole and external beveling (white arrow head), **c** Synbone® femur cylinder with a square exit hole, external beveling (black arrow head) and internal beveling (white arrow head), **d** Synbone® humerus cylinder with a round exit hole and external beveling (white arrow head), **e** deer femur with external beveling (black arrow head) and internal beveling (white arrow head).

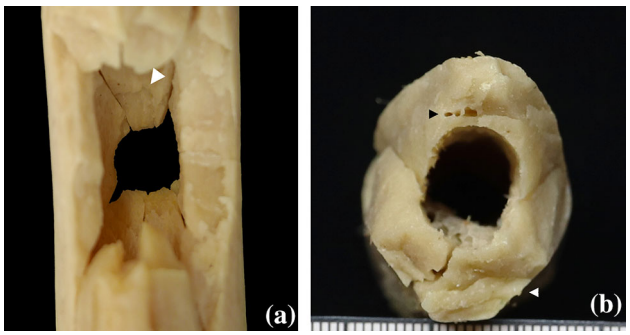

Figure 3 **a** The exit side of a human femur with the view on internal entrance beveling (white arrow head), and **b** axial view on the fracture surface of a human femur showing wall splitting (black arrow head) at the impact side and layered breakage (white arrow head) at the exit side.

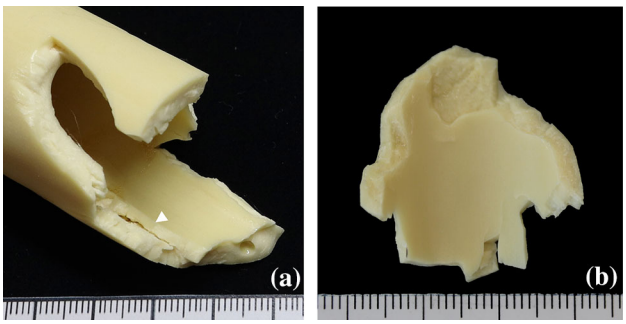

Figure 4 **a** Oblique-lateral view on a Synbone® femur cylinder with wall splitting (white arrow head) and a void lacuna in the material, and **b** demonstrates the irregular fragment shape of a Synbone® humerus cylinder.

reconstructed. Layered breakage occurred in all human femurs and the majority of human humeri. This finding is statistically significant, since it was never featured by the Synbone® surrogates and the animal bones. No significant differences were found for external beveling and radiating fracture lines. External beveling was present in all specimens with the exception of one femur cylinder from Synbone®. Radiating fracture lines were present in all samples.

General traits

Plastic deformation is a persistent deformation of bone.

Wall splitting is a separation of bone within the cortical wall (Figs. 3, 4).

Plastic deformation was present in all human and animal samples. This finding is significantly significant, since in the Synbone® surrogates it never occurred. Wall splitting was significantly more frequent in both Synbone® models compared to human femurs. In human humeri and deer femurs it was never observed.

Multivariate analysis

All qualitative variables were used for a multivariate correspondence analysis (Fig. 5). The results showed that human bones and Synbone® surrogates feature distinctive fracture patterns. A closer inspection shows two clusters of fracture patterns, one typically found in human bones and the other in Synbone® surrogates. The cluster of typical ballistic traits

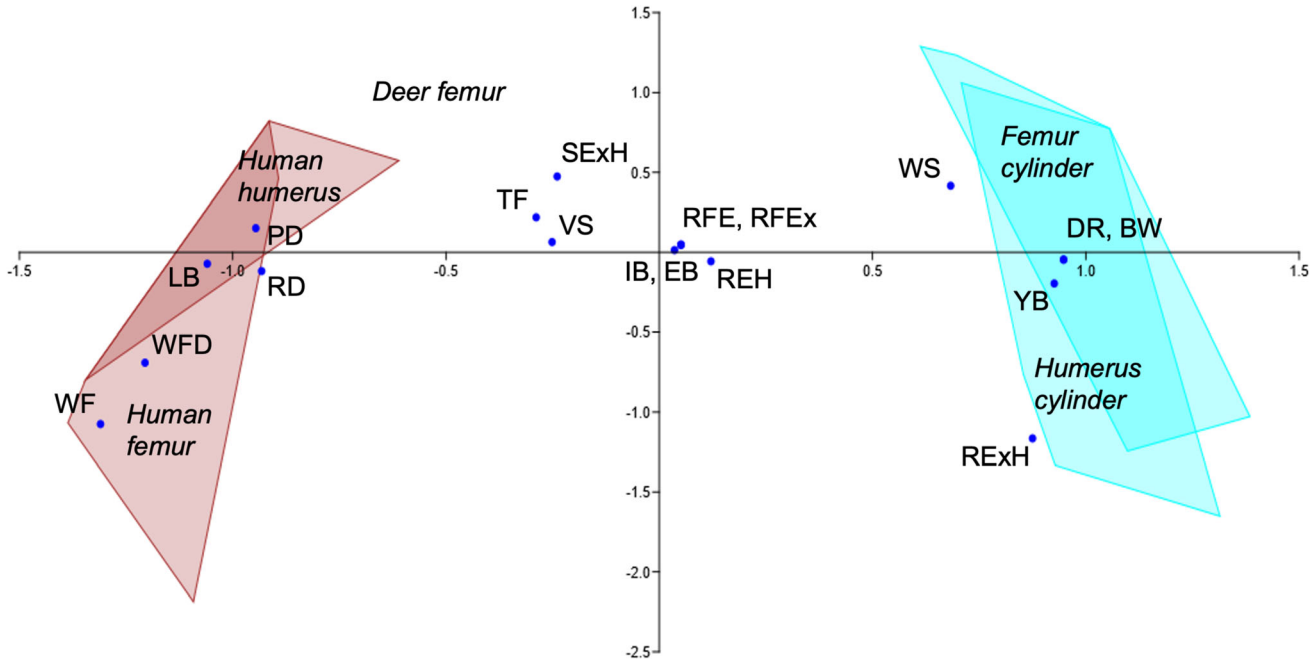

Figure 5 The multivariate correspondence analysis with the qualitative cortical traits evaluated in all sample groups (REH = round entrance hole, VS = V-shape, YB = Y-branching, TF = tip fragmentation, WF = wing flake, WFD = wing flake defect, RD = ring defect, DR = depressed ring, BW = bullet wipe, IB = internal beveling, RFE = radiating fracture lines entrance, RExH = round exit hole, SExH = square exit hole, LB = layered breakage, EB = external beveling, RFEx = radiating fracture lines exit, PD = plastic deformation, WS = wall splitting). The first component represents 52% of the total variance and the second component 14%, cumulative both axes represent 66%.

observed in human bones consists of ring defect, wing flake, wing flake defect, layered breakage and plastic deformation. The cluster of typical ballistic traits observed in Synbone® surrogated consists of depressed ring, bullet wipe, Y-branching, round exit hole and wall splitting. The cluster of cortical traits featured by the animal model is more similar to the cluster reproduced in human bones.

Quantitative fracture characteristics

The entry and exit hole diameters, fracture extent, and the presence of transverse fracture lines could only be evaluated for the human and Synbone® specimens (Table 2; Fig. 6). The largest mean fracture extent was found in human femurs. Statistically significant differences were found compared to the human humeri and femur cylinders. Furthermore, among the humerus cylinders a considerable variation of the fracture extent was observed.

The entry and exit holes were measured in their vertical and horizontal diameter. Compared to the projectile's diameter, the mean vertical entry hole diameter in human bones and humerus cylinders was larger, while in femur cylinders it was smaller. Comparing the sample groups, the mean vertical diameter in the femur cylinders were significantly smaller than in the other three sample groups. The mean horizontal entry hole diameter in human bones was larger, while in Synbone® surrogates it was smaller than the projectile's diameter. Comparing the sample groups, the mean horizontal diameter in human bones was significantly bigger than in the Synbone® surrogates. Among the Synbone® surrogates the horizontal diameter in humerus cylinders were significantly bigger than in femur cylinders. The mean vertical exit hole diameter in human humeri was significantly bigger than in all other three sample groups. The mean horizontal diameter was significantly bigger in femur cylinders compared to human bones and in humerus cylinders compared to human humeri.

The percentage of transverse, oblique and longitudinal fracture lines compared to all entrance associated radiating fracture lines are shown in Table 2. Statistical differences were found for the percentage of transverse fracture lines that was significantly

Table 2 Descriptive statistics of the entry and exit hole size (VD = vertical diameter, HD = horizontal diameter), fracture extent, percentage of the transversal, oblique and longitudinal fracture lines out of the entrance associated fracture lines in human bones and Synbone® surrogates

Quantitative variables	Group	*N*	Mean	SD	Min	Max
Entry hole VD (mm)	FH	7	10.4	1	9	11.5
	HH	7	10	0.7	9	11
	FS	10	8.3	0.4	8	9
	HS	10	9.8	0.5	9	11
Entry hole HD (mm)	FH	7	10.4	0.5	10	11
	HH	7	9.8	0.9	9	11
	FS	10	6.8	0.3	6.5	7
	HS	10	8.6	0.5	8	9
Exit hole VD (mm)	FH	7	16	3.9	12.5	23
	HH	7	24.7	10	13.5	40.5
	FS	10	15.4	4.3	8.5	22
	HS	10	14.2	4.4	11	24.5
Exit hole HD (mm)	FH	7	11.2	1.6	9	13
	HH	7	9.5	1.7	8	12.5
	FS	10	13.8	1.8	11	16
	HS	10	12.9	2.1	10	15.5
Fracture extent (cm)	FH	7	14.2	2.6	11.2	17.9
	HH	7	9.5	1.8	6.5	12.0
	FS	10	10.2	2.4	6.9	15.1
	HS	10	11.1	3.8	6.7	16.6
Transverse Fx lines (%)	FH	7	8.7	8.4	0	17
	HH	7	10.3	10.9	0	29
	FS	10	24.5	4.3	18	33
	HS	10	22.2	8.4	11	33
Oblique Fx lines (%)	FH	7	83.7	16.9	50	100
	HH	7	73.4	11.4	57	86
	FS	10	64.1	10.5	50	78
	HS	10	68.3	10.7	50	88
Longitudinal Fx lines (%)	FH	7	7.6	13.6	0	33
	HH	7	16.3	12.8	0	33
	FS	10	11.5	10.9	0	25
	HS	10	9.6	9.8	0	25
Energy loss (J)	FH	4	352.4	29.9	316.9	389.1
	HH	6	232.4	29.8	193.8	265.7
	FS	10	168.3	10.7	153.4	188.7
	HS	10	124.8	12	108.9	151.1
	FA	4	245.5	32.4	215.2	278.6

Also shown is the projectile's energy lost upon impact in all five sample groups (*FH*, human femur, *HH*, human humerus, *FS*, femur cylinder, *HS*, humerus cylinder, *FA*, deer femur)

higher in both Synbone® surrogates compared to human femurs (Fig. 6). No significant differences were found for the presence of oblique and longitudinal fracture lines.

The projectile's exit velocity was detected in all samples, except in three human femurs and one humerus due to interferences. Table 2 and Fig. 7 show the calculated energy loss upon impact in all sample groups. The mean energy loss in the human femur was significantly higher than in the rest of sample groups. Energy loss in the human humeri was significantly higher than in both Synbone® surrogates. Energy loss in the deer femurs was most similar to human humeri. It was significantly higher than in the humerus cylinders from Synbone®. Furthermore, also between the two Synbone® models, the energy loss in femur cylinders were significantly higher than in humerus cylinders.

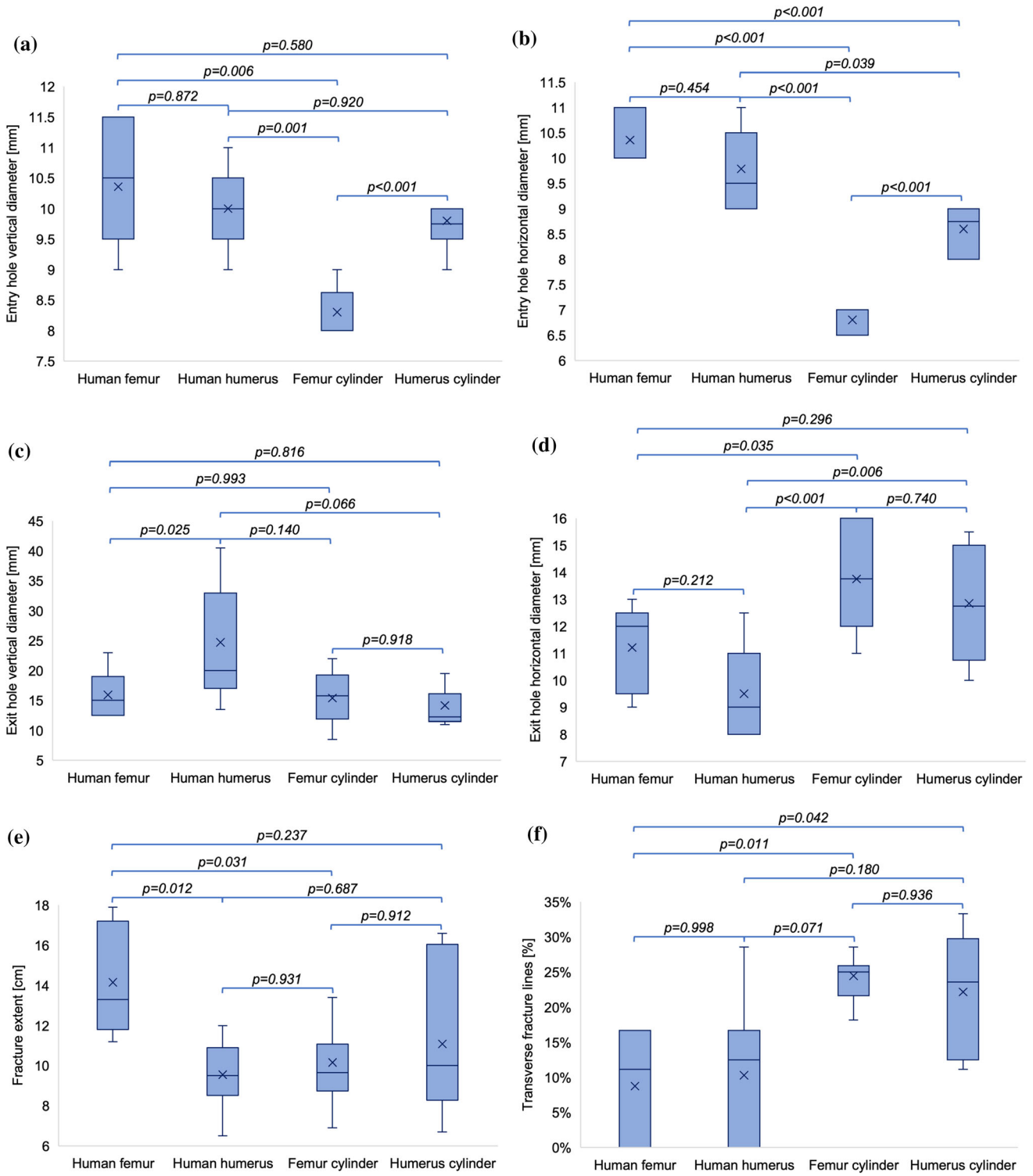

Figure 6 Box plots representing the **a** vertical and **b** horizontal entry hole diameter, the **c** vertical and **d** horizontal exit hole diameter, the **e** fracture extent, and **f** the percentage of transverse fracture lines out of the entrance associated fracture lines in human bones and Synbone® surrogates (*p*-values for the pairwise comparison).

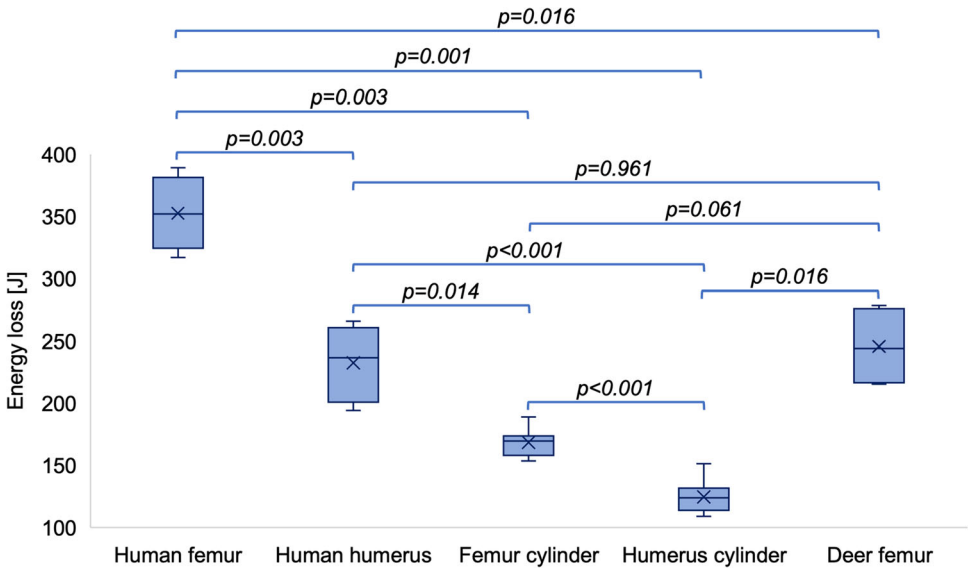

Figure 7 Box plots representing the projectiles' energy lost upon impact in all five sample groups (*p*-values for the pairwise comparison).

Discussion

Alternative models for trauma experiments are of great interest due to the restricted possibilities of using human specimens for forensic research. Despite different tissue and material, a suitable alternative is thought to exhibit properties such as elasticity, strength and energy absorption similar to human tissue [32]. Moreover, useful models should ensure reproducibility [12]. To date, this is the first experimental study designed to provide conclusions on whether Synbone® cylinders and deer femurs are suitable to macroscopically reproduce detailed ballistic fracture patterns in human long bones. For this purpose, we shot with real ammunition and used real human bones as a comparison alongside the alternative synthetic and animal models.

The macroscopical generalization of the fractures

On the first sight, the ballistic fractures in each sample group appeared similar. All samples presented comminuted fracture, which is consistent with the review by Veenstra et al [22]. revealing comminuted fracture is the most frequent diaphyseal fracture in gunshot trauma. In order to characterize the fracture type more accurately, we considered the appearance at the impact side. Stellate fracture was identified in all sample groups, as it has also been observed by other authors [11, 21, 28, 34]. All models allowed the assessment of the impact direction and bullet trajectory, since entrance and exit side could be identified and distinguished from each other. Interestingly, some authors revealed that the exit hole is not always present in long bones because the bullet entry fragments the bone before the projectile reaches the other side of the shaft [21, 35]. This observation could not be made in our study. In all sample groups, we found a beveled exit with radiating fracture lines allowing the conclusion that they were directly produced by the projectile. Certainly, the entrance associated fracture lines that reach the posterior aspect may influence the shape of the exit fracture, taking into account the Puppe rule that fracture lines stop at preexisting ones [36]. As a standard feature to distinguish between entrance and exit, it is well known that bone bevels out in the direction in which the projectile travels [34]. In cranial bones, the entry wound classically presents an internal beveling, whereas external beveling is a typical characteristic of the exit wound [37, 38]. In our study, internal beveling of the entrance defect and the already mentioned external beveling of the exit defect were reproduced in all sample groups. Furthermore, in all sample groups the exit fractures were dominated by a vast fragmentation and thus larger than the bullet entry as it has already been reported in human long bones [39]. In accordance with claims about the particular importance of the entry wound assessment [40], we found the impact side in all sample groups provided more characteristic traits to identify gunshot trauma than the exit side.

The fracture macroscopy in detail

A detailed fracture pattern analysis showed that both the surrogate and animal models differed significantly from human bones. When comparing the two alternative models, the clusters of entry, exit, and general cortical traits in the animal model were found to be more similar to human bone than the Synbone® surrogates.

In a ballistic study comparing human craniums with Synbone® plates and spheres, Smith et al. [41] noted similar entry but different exit wound features between the models. Unlike these findings, in our long bone models especially the entrance fracture presented differences between the sample groups. We observed traits that revealed to be distinct for human bones and described them as wing flake, wing flake defect and ring defect. The aspect of V-shape, as already observed by Martrille et al. [21], and tip fragmentation, a term we defined in this study, were reproduced in all sample groups. However, both traits appeared significantly more often in human and animal bones than in Synbone® surrogates. Y-branching, depressed ring and bullet wipe revealed to be characteristic Synbone® entrance traits. According to the literature, the presence or absence of a depressed ring may help to identify the type of ammunition in terms of fully jacket or lead bullets [25, 42]. However, this finding may not be applicable in human bones, since we could not reproduce it there. Another unique Synbone® finding is the bullet wipe that may be associated with the presence of a depressed ring. With other words, in Synbone® we found the anterior surface around the bullet entry depressed but mostly intact. In contrast, in human and animal bones we always saw a loss of cortical bone around the bullet entry. The main difference on the impact side of the deer femurs was that especially the medial and lateral aspects of the bullet entry were shattered and could not be reassembled. This did not allow us the same precise evaluation of the entrance traits compared to human bones and Synbone® surrogates.

With respect to the exit fracture, we also found some dissimilarities between the three models. Layered breakage revealed to exclusively occur in human bones. Interestingly, this trait has formerly been associated to the compression side of blunt force trauma in fresh human long bones [33]. The Synbone® femur cylinders mostly presented a square hole like in human bones, whereas the majority of the humerus cylinders showed a round exit hole. The deer bones did not allow the assessment of the exit shape.

In terms of general cortical traits, exclusively the real bones featured plastic deformation which is referred as to the persistent deformation of bone prior fracturing [34]. In contrast, wall splitting revealed to be a distinct Synbone® trait.

Focusing on caliber estimation, studies on cranial bones have revealed that the minimum diameter of the entry hole allows the discrimination between "small" and "large" calibers, whereas a precise determination is difficult [43–45]. In our study, we found significant differences between the entry size in the models. The human bones reproduced bigger entry holes, while the Synbone® surrogates featured mostly smaller entry holes than the projectile used. This may be explained by the different entry hole traits, ring defect in human bones versus depressed ring in Synbone® surrogates. While the first represents a cortical loss of bone, the latter can be regarded as an inward folding of the material. Again, the deer bones could not be used to evaluate the entry hole size.

The energy loss of the projectile upon impact

Our results on the bullet's energy lost upon impact indicates that the resistance to the projectile is significantly lower in Synbone® cylinders than in human and deer bones. Interestingly, this result differs from the finding that Synbone® surrogates feature a similar resistance to porcine bone [24, 25].

In accordance with the literature, the distinct fracture patterns found in our study may essentially be attributed to differences in the underlying material [25, 41]. In respect of the microstructural differences, it has been expressed that polyurethane is not a suitable alternative for studies investigating bone trauma below a very general and superficial level [41]. Thus, other authors have argued that animal bones remain an essential alternative model for human bone trauma [46].

Surrogate material such as polyurethane does not feature the microstructural complexity of real bone based on its components and their arrangement in space [47]. Despite some histological differences between the species [48, 49], all bones consist of a

mineral phase (hydroxyapatite) embedded in an organic matrix (mainly type I collagen). The former makes the bone rigid and stiff, while the latter contributes to its toughness and gives it a certain flexibility reducing brittleness and allowing some resistance to fracture [50]. Also, the water content is critical to the mechanical behavior [34]. Bone is a fluid-imbibed material and its water is not only present in the vascular system and canaliculi, but also structurally bound in the collagen matrix [51]. It was found that drying out of a bone is related to a loss of elasticity and plasticity [33, 52]. In this context, fracture characteristics have been linked to the elasticity, cohesiveness and density of bone [53]. It is known that the less flexible the tissue the greater the damage because more energy is transferred to the stretch mechanism [54, 55].

But, not only intrinsic factors influence the bone's fracture biomechanics. It is thought that in response to different mechanical stressors bone reacts differently. In blunt force trauma, bone has been observed to behave like a ductile material by deforming prior to fracturing [33]. In contrast, in gunshot trauma, bone typically behaves as a stiff and brittle material and tends to fracture instantly before deformation can occur [56]. These authors, however, do not provide information on the impact speed. In our study, simulating a shot from a pistol, we could find plastic deformation in all human and deer bones. Indeed, this finding finds support by the observation of Martrille et al. [21] who also reported on the occurrence of plasticity prior fracturing in gunshot trauma. In the Synbone® models we could not find plastic deformation. A potential explanation is that the surrogates may are more brittle than real bone. Further support for this is given by our finding that transverse fractures occurred more frequently in the Synbone® surrogates than human bones. In the literature, transverse lines are typical associated to fractures in dry, brittle bone [57].

In our study, the deer femurs were massively fragmented into very small pieces and chips. The fracture could not be as efficiently reconstructed and thus not all parts as precisely evaluated as human bones and Synbone® cylinders. We considered this as a main drawback of the animal model. Interestingly, this finding differs from results by Kieser et al. [28] who found radiating fracture lines producing a butterfly-shaped fracture at the impact side of the anterior mid-shaft of fresh mature female deer femurs. Compared to our study, their findings resemble more the fracture pattern found in our human bones than in our deer bones. We assume that this difference may be particularly traced back to the impact energy of 0.013–5.35 J of the spherical steel projectiles used in the experiments by Kieser, compared to the impact energy of 517.97 J in our study. This assumption may be supported by the literature reporting bone behaves more like brittle material under high velocity impacts [58, 59]. Since the grade of comminution is not only associated to the amount of transferred energy but also to a small target size [34], an additional influence might be related to the smaller size of the deer bones used in our study (Iberian subspecies from Catalonia, Spain). They featured an average length of 22.4 cm and an average diaphyseal width of 1.9. We assume they were smaller than the ones used by Kieser et al. [27] from New Zealand, who reported in an earlier study an average bone length of 27.6 cm and a mid-diaphyseal width of 2.7 cm. The relation between the grade of comminution and a small target size may further be supported by our experience that human humeri compared to human femurs shattered in smaller fragments and hence were more difficult to assemble. Kieser et al. reported deer femurs being a suitable model to substitute human femurs. The deer femurs used in our study were considerably smaller and from this point of view they might rather substitute human humeri. This can find further support by our observation that energy loss in human humeri and deer femurs were quite similar. With respect to the material properties, the deer bones seem to have a comparable toughness as human humeri.

Ultimately, an additional explanation for the different fracture patterns found in our study may constitute the geometrical variability of the models, in particular dissimilar cortical thickness and the complex shape of real bone. In accordance with Smith et al. [41], these factors also influence the resistance through thinner and thicker bone areas and thus fracture propagation. As noted, there is no animal bone that geometrically resembles a human femur or humeri. In case of the Synbone® surrogates, there exist anatomical models, however the ones especially developed for ballistic testing were geometrically simplified. These simplified cylinders have been developed to reduce the effect of heterogeneous tissues during research and hence should guarantee reproducibility. In this context, however, we could observe some differences in the detailed fracture

patterns among the Synbone® models. Some entrance traits such as V-shape, Y-branching, Tip fragmentation and ring defect only occurred irregularly. Also the exit hole reveled to appear round or square shaped. Furthermore, we found a considerable variability of the fracture extent among of the humerus cylinders. In contrast to the findings of Henwood et al. [25], however, we did not observe fractures reaching the cut edges of the cylinders. Since fracture lines run along the least resistance [9], a potential explanation for the observed inconsistencies among the Synbone® models may lay in a certain degree of heterogeneity of the polyurethane wall. As an indicator for this heterogeneity, we found void lacunas of up to 2.5 mm in some samples. This assumption finds further support by our observation of irregular fragment shapes in the Synbone® models. Henwood et al. [25] made an analogous observation, reporting on a sudden change of fracture direction in Synbone® surrogates that could not be observed in real bones from pigs. The authors claimed that the fracture lines change the direction when they reached a different pore density. However, they also express some reluctance to accept this interpretation because not all fracture lines showed a response to the change in pore density.

Limitations

A limitation of the research presented in our study may concern the sample size, in particular the number of animal bones. However, within this groups we found a 100% congruence of the presence or absence of the evaluated fracture patterns. Furthermore, the results of this study represent fracture patterns in the diaphysis, produced by a 9 mm full metal jacket projectile with an impact speed of 360 m/s. Gunshot trauma in more cancellous rich areas such as the epiphyses as well as different bullet types and impact velocities may produce different fracture patterns. Since the scope of this study was only a macroscopical evaluation, it might be useful to investigate the material behavior of each model from a microstructural point of view.

Conclusion

The ballistic fracture patterns produced in the Synbone® surrogates and animal bones tested in this study were a fair general approximation of those seen in human long bones. However, a detailed analysis revealed a range of dissimilarities that calls caution in extrapolating ballistic fracture patterns of alternative models to human long bones. The Synbone® surrogates did not present all the observed human fracture traits and in addition, they presented different characteristics. This leads to the conclusion that the polyurethane material provides an alternate failure mechanism than real bone. The animal model tested in our study revealed to be more suitable than Synbone®, in terms of both qualitative and quantitative fracture characteristics. However, the main drawback of the deer femurs was the massive fragmentation that did not allow us the same precise fracture reconstruction as in human bone and Synbone® surrogates. Our study shows that special caution is needed when validating surrogate material with animal bone instead of human bone. We further emphasize the continued need for innovation in new model systems such as computational modeling. However, before alternative models can be validated, further experiments with real human long bones seem to be required to define a distinct ballistic fracture pattern.

Acknowledgements

Funding support for the current project was provided by the Research Fund for Excellent Junior Researchers of the University of Basel, Switzerland. A very special thank goes to Professor Christian De Geyter, Professor Eva Scheurer and Professor Roland Hausmann. We are extremely grateful for the collaboration with the Mossos d'Esquadra for providing the facilities, the material and the personal staff.

Authors' contribution

Conceptualization was contributed by NS and IG; Methodology was contributed by NS, JS, XG, PB, AS, and MO-S; Formal analysis and investigation were contributed by NS, IG, and XJ; Writing—original draft preparation was contributed by NS; Writing—

review and editing was contributed by IG, XJ, and NS; Visualization was contributed by NS, IG, and XJ; Supervision was contributed by IG and XJ.

Funding

Open Access Funding provided by Universitat Autonoma de Barcelona.

Data availability

The data generated during and/or analyzed during the current study are available from the corresponding author on reasonable request.

Declarations

Conflict of interest The authors have no conflicts of interest to declare that are relevant to the content of this article.

Ethics approval This study followed the ethical precepts of the Declaration of Helsinki (Fortaleza, Brazil, Oct 2013) and was approved by local ethics committee (Bellvitge University Hospital, L'Hospitalet de Llobregat, Barcelona; Ref. PR416/20). Human samples were processed according to guidance for clinical use (EEC regulations 2004/23/CE and 2006/17/CE) and to the legal requirements Spain (Law 14/2007, RD 1716/2011 and RD 9/2014). All human bone samples were donated anonymously and obtained under informed consent. The respective samples are stored in the private collection at the IMLCFC (Barcelona, Spain) (Registro Nacional de Biobancos. Ref. C.0004241).

References

[1] Saukko P, Knight B (2015) Knight's forensic pathology. CRC Press, Boca Raton

[2] Sorg MH, Haglund WD (eds) (1996) Forensic taphonomy: the postmortem fate of human remains. CRC Press, Boca Raton

[3] Andrews P, Fernández-Jalvo Y (2012) How to approach perimortem injury and other modifications. Forensic microscopy for skeletal tissues. Humana Press, Totowa, pp 191–225

[4] Cappella A, Castoldi E, Sforza C, Cattaneo C (2014) An osteological revisitation of autopsies: comparing anthropological findings on exhumed skeletons to their respective autopsy reports in seven cases. Forensic Sci Int 244:315-e1

[5] Sauer NJ (1998) The timing of injuries and manner of death: distinguishing among antemortem, perimortem and postmortem trauma. Forensic Osteol: Adv Identif Hum Remains 2:321–331

[6] Hart GO (2005) Fracture pattern interpretation in the skull: differentiating blunt force from ballistics trauma using concentric fractures. J Forensic Sci 50(6):1–6

[7] Symes SA, Ericka N, L'Abbé ENC, Wolff I, Dirkmaat DC (2012) 17 interpreting traumatic. Companion Forensic Anthropol 39:340

[8] O'BC S, Berryman HE, Lahren CH (1987) Cranial fracture patterns and estimate of direction from low velocity gunshot wounds. J Forensic Sci 32(5):1416–1421

[9] Berryman HE, Symes SA (1998) Recognizing gunshot and blunt cranial trauma through fracture interpretation. Forensic Osteol: Adv Identif Hum Remains 2:333–352

[10] Smith OC, Pope EJ, Symes SA (2015) Look until you see: identification of trauma in skeletal material. Hard evidence. Routledge, Abingdon, pp 190–204

[11] Bland-Sutton J (1915) Observations on injuries of the bones of the limbs by the S Bullet. BMJ Mil Health 24(4):314–323

[12] Bir C, Andrecovich C, DeMaio M, Dougherty PJ (2016) Evaluation of bone surrogates for indirect and direct ballistic fractures. Forensic Sci Int 261:1–7

[13] Huelke DF, Buege LJ, Harger JH (1967) Bone fractures produced by high velocity impacts. Am J Anat 120(1):123–131

[14] Huelke DF, Harger JH, Buege LJ, Dingman HG, Harger DR (1968) An experimental study in bio-ballistics: femoral fractures produced by projectiles. J Biomech 1(2):97–105
[15] Huelke DF, Harger JH, Buege LJ, Dingman HG (1968) An experimental study in bio-ballistics: femoral fractures produced by projectiles—II shaft impacts. J Biomech 1(4):313–321
[16] Dougherty PJ, Sherman D, Dau N, Bir C (2011) Ballistic fractures: indirect fracture to bone. J Trauma Acute Care Surg 71(5):1381–1384
[17] Berryman HE, Gunther WM (2000) Keyhole defect production in tubular bone. J Forensic Sci 45(2):483–487
[18] Dougherty PJ, Vaidya R, Silverton CD, Bartlett C, Najibi S (2009) Joint and long-bone gunshot injuries. JBJS 91(4):980–997
[19] Long WT, Chang W, Brien EW (2003) Grading system for gunshot injuries to the femoral diaphysis in civilians. Clin Orthop Relat Res 1976–2007(408):92–100
[20] Ryan JR, Hensel RT, Salciccioli GG, Pedersen HE (1981) Fractures of the femur secondary to low-velocity gunshot wounds. J Trauma 21(2):160–162
[21] Martrille L, Symes SA (2019) Interpretation of long bones ballistic trauma. Forensic Sci Int 302:109890
[22] Veenstra A, Kerkhoff W, Oostra RJ, Galtés I (2022) Gunshot trauma in human long bones: towards practical diagnostic guidance for forensic anthropologists. Forensic Sci Med Pathol 18:1–9
[23] Synbone® (2022) Portfolio for ballistic testing. https://www.synbone.com/product-category/biomechanics-generics/forensic-and-ballistic/forensic-and-ballistic-rod/?shop_currency=CHF. Accessed 10 Oct 2022
[24] Kneubuehl BP, Thali MJ (2003) The evaluation of a synthetic long bone structure as a substitute for human tissue in gunshot experiments. Forensic Sci Int 138(1–3):44–49
[25] Henwood BJ, Appleby-Thomas G (2020) The suitability of Synbone® as a tissue analogue in ballistic impacts. J Mater Sci 55:3022–3033. https://doi.org/10.1007/s10853-019-04231-y
[26] Kieser DC, Carr DJ, Leclair SCJ, Horsfall I, Theis JC, Swain MV, Kieser JA (2013) Gunshot induced indirect femoral fracture: mechanism of injury and fracture morphology. BMJ Mil Health 159(4):294–299
[27] Kieser DC, Carr DJ, Leclair SC, Horsfall I, Theis JC, Swain MV, Kieser JA (2013) Clothing increases the risk of indirect ballistic fractures. J Orthop Surg Res 8(1):1–7
[28] Kieser DC, Riddell R, Kieser JA, Theis JC, Swain MV (2014) Bone micro-fracture observations from direct impact of slow velocity projectiles. J Arch Mil Med 2(1):1–6
[29] Zhang X, Xu C, Wen Y, Luo S (2015) The experimental and numerical study of indirect effect of a rifle bullet on the bone. Forensic Sci Int 257:473–480
[30] Kieser DC, Kanade S, Waddell NJ, Kieser JA, Theis JC, Swain MV (2014) The deer femur—a morphological and biomechanical animal model of the human femur. Bio-Med Mater Eng 24(4):1693–1703
[31] Jussila J (2005) Wound ballistic simulation: assessment of the legitimacy of law enforcement firearms ammunitionby means of wound ballistic simulation. Academic Dissertation, University of Helsinki
[32] Kneubuehl BP, Coupland RM, Rothschild MA, Thali MJ (2011) Wound ballistics: basics and applications. Translation of the 3rd German edition. Springer, Berlin
[33] Scheirs S, Malgosa A, Sanchez-Molina D, Ortega-Sánchez M, Velázquez-Ameijide J, Arregui-Dalmases C, Medallo-Muñiz J, Galtés I (2017) New insights in the analysis of blunt force trauma in human bones. Preliminary results. Int J Legal Med 131(3):867–875
[34] Kieser J, Taylor M, Carr D (2012) Forensic biomechanics. Wiley, Hoboken
[35] Smith OC, Pope EJ, Symes SA (2015) Look until you see: identification of trauma in skeletal material. In: Hard evidence. Routledge
[36] Madea B, Staak M (1988) Determination of the sequence of gunshot wounds of the skull. J Forensic Sci Soc 28(5–6):321–328
[37] Quatrehomme G, Işcan MY (1998) Analysis of beveling in gunshot entrance wounds. Forensic Sci Int 93(1):45–60
[38] Quatrehomme G, İşcan MY (1997) Bevelling in exit gunshot wounds in bones. Forensic Sci Int 89(1–2):93–101
[39] Huelke D, Darling J (1964) Bone fractures produced by bullets. J Forensic Sci 9(4):461–469
[40] DiMaio VJ (2015) Gunshot wounds: practical aspects of firearms, ballistics, and forensic techniques. CRC Press, Boca Raton
[41] Smith MJ, James S, Pover T, Ball N, Barnetson V, Foster B, Guy C, Rickman J, Walton V (2015) Fantastic plastic? Experimental evaluation of polyurethane bone substitutes as proxies for human bone in trauma simulations. Legal Med 17(5):427–435
[42] Henwood B, Oost T, Fairgrieve S (2019) Bullet caliber and type categorization from gunshot wounds in *Sus scrofa* (Linnaeus) long bone. J Forensic Sci. https://doi.org/10.1111/1556-4029.14004
[43] Berryman H, Smith O, Symes S (1995) Diameter of cranial gunshot wounds as a function of bullet caliber. J Forensic Sci 40(5):751–4
[44] Ross A (1996) Caliber estimation from cranial entrance defect measurements. J Forensic Sci 41(4):629–33

[45] Paschall A, Ross A (2017) Bone mineral density and wounding capacity of handguns: implications for estimation of caliber. Int J Legal Med 131(1):161–6

[46] Muschler GF, Raut VP, Patterson TE, Wenke JC, Hollinger JO (2010) The design and use of animal models for translational research in bone tissue engineering and regenerative medicine. Tissue Eng Part B Rev 16(1):123–145

[47] Augat P, Schorlemmer S (2006) The role of cortical bone and its microstructure in bone strength. Age Ageing 35(-suppl_2):ii27–ii31

[48] Hillier ML, Bell LS (2007) Differentiating human bone from animal bone: a review of histological methods. J Forensic Sci 52(2):249–263

[49] Dominguez VM, Crowder CM (2012) The utility of osteon shape and circularity for differentiating human and non-human Haversian bone. Am J Phys Anthropol 149(1):84–91

[50] Wang X, Shen X, Li X, Agrawal CM (2002) Age-related changes in the collagen network and toughness of bone. Bone 31(1):1–7

[51] Nyman JS, Roy A, Shen X, Acuna RL, Tyler JH, Wang X (2006) The influence of water removal on the strength and toughness of cortical bone. J Biomech 39(5):931–938

[52] Pineri MH, Escoubes M, Roche G (1978) Water–collagen interactions: calorimetric and mechanical experiments. Biopolym: Orig Res Biomol 17(12):2799–2815

[53] Schmitt KU, Niederer PF, Cronin DS, Morrison B III, Muser MH, Walz F (2019) Trauma biomechanics: an introduction to injury biomechanics. Springer, Cham

[54] Sellier KG, Kneubuehl BP, Haag LC (1995) Wound ballistics and the scientific background. Am J Forensic Med Pathol 16(4):355

[55] Fackler ML (1996) Gunshot wound review. Ann Emerg Med 28(2):194–203

[56] Özkaya N, Nordin M (1999) Fundamental of biomechanics: equilibrium, motion and deformation, 2nd edn. Springer, New York, pp 17–21, 125–147, 206–210

[57] Wheatley BP (2008) Perimortem or postmortem bone fractures? An experimental study of fracture patterns in deer femora. J Forensic Sci 53(1):69–72

[58] Einhorn TA (1992) Bone strength: the bottom line. Calcif Tissue Int 51(5):333–339

[59] Cohen H, Kugel C, May H, Medlej B, Stein D, Slon V, Hershkovitz I, Brosh T (2016) The impact velocity and bone fracture pattern: forensic perspective. Forensic Sci Int 266:54–62